

MSc Thesis Presentation

Digital Treatment of Signals from a triple – alpha source

Maria-Magdalini Satrazani

Supervisor: prof. Benoît Gall

June 2020,
Strasbourg

Université

de Strasbourg



Outline

- Introduction
 - S3 Spectrometer
 - SIRIUS Detection System
 - The Tunnel Detector for SIRIUS
 - The Test Bench at IPHC
 - The TNT2 Card
 - The Jordanov Algorithm
- Results
 - Formation of Jordanov Signals
 - Role of M
 - Role of τ
 - Tau Histograms
 - Amplitude Histograms
 - Energy Calibration
- Conclusion
- References

Introduction – S3 Spectrometer

- S3 is designed in order to provide great selectivity and rejection of nuclei delivered by a *LINAC*, which is a radioactive linear beam accelerator and part of the SPIRAL2 Project, located at GANIL laboratory in Caen.

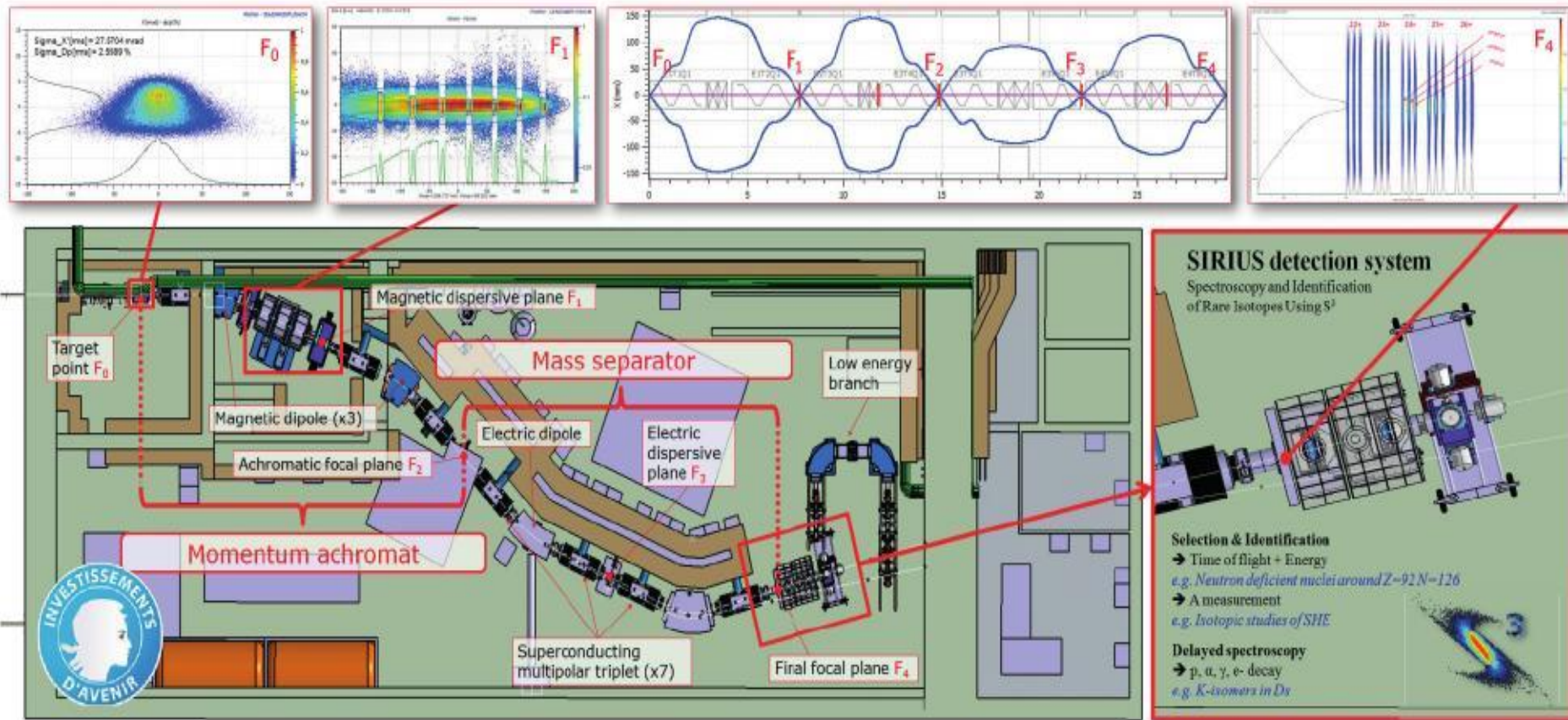


Figure 1. The experimental room with all the S3 components. / IPHC site, S3 collaboration.

Introduction – SIRIUS Detection System

- The nuclei of interest meet several detectors before they are finally implanted into the DSSD detector. We are interested only in the *Tunnel Detector*.

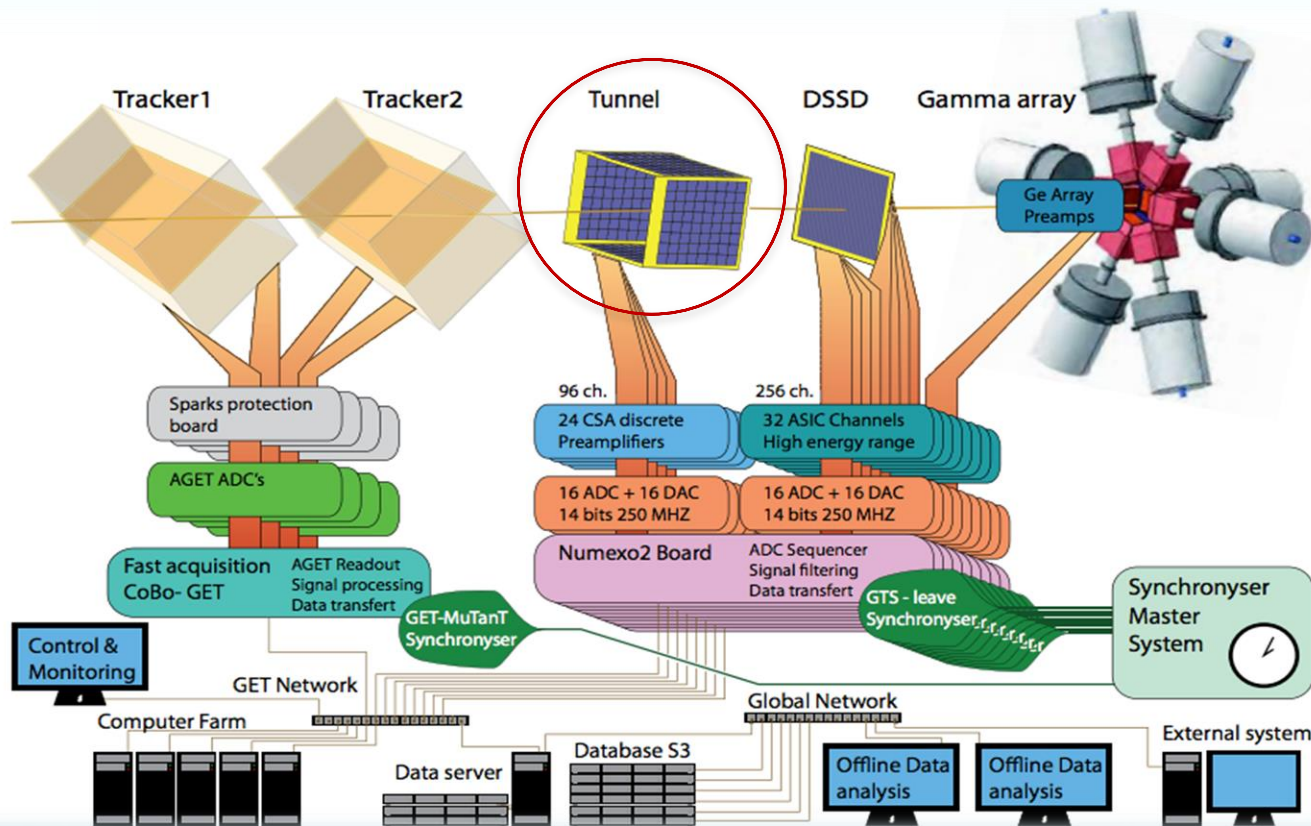


Figure 2. The SIRIUS detection system. From left to right: the trackers, the tunnel, the DSSD and the Ge detectors. Under the detectors they are schematized the different elements of the electronic acquisition of the corresponding signals. / Hugo Faure, Thèse, Développement et validation d'un nouveau détecteur silicium de grande taille pour S3-SIRIUS

Introduction – The Tunnel Detector for SIRIUS

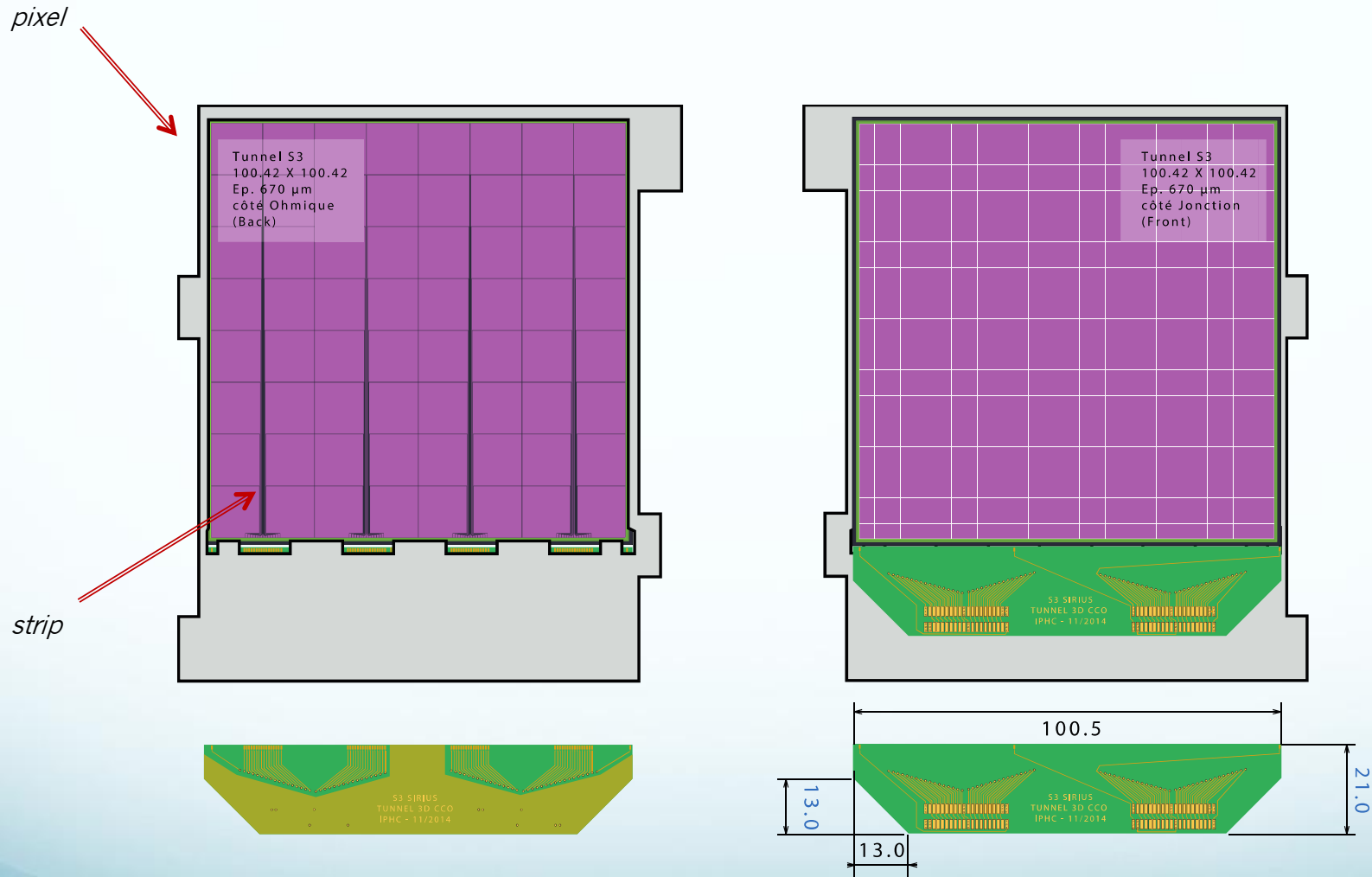


Figure 3. Schematic layout of the Stripy Pad detector: on the left is the ohmic side composed of 64 pixels, on the right is the junction side of the detector composed only from one large pixel. / Courtesy of Benoît Gall

Introduction – The Test Bench at IPHC

- It can provide us with electrical signals resulting from the interaction of α – particles with Silicon.
- From their analysis we can interpret the properties of the pulses and the functionality principle of the *Tunnel detector*.



Figure 4. The Test Bench at IPHC in Strasbourg. /Courtesy of Benoît Gall.

Introduction– The TNT2 Card

- They are sampling the signal at *100 MHz*.
- They use the analog signal from the preamplifier as an input, and in the output they give digital traces that are later processed by an algorithm.

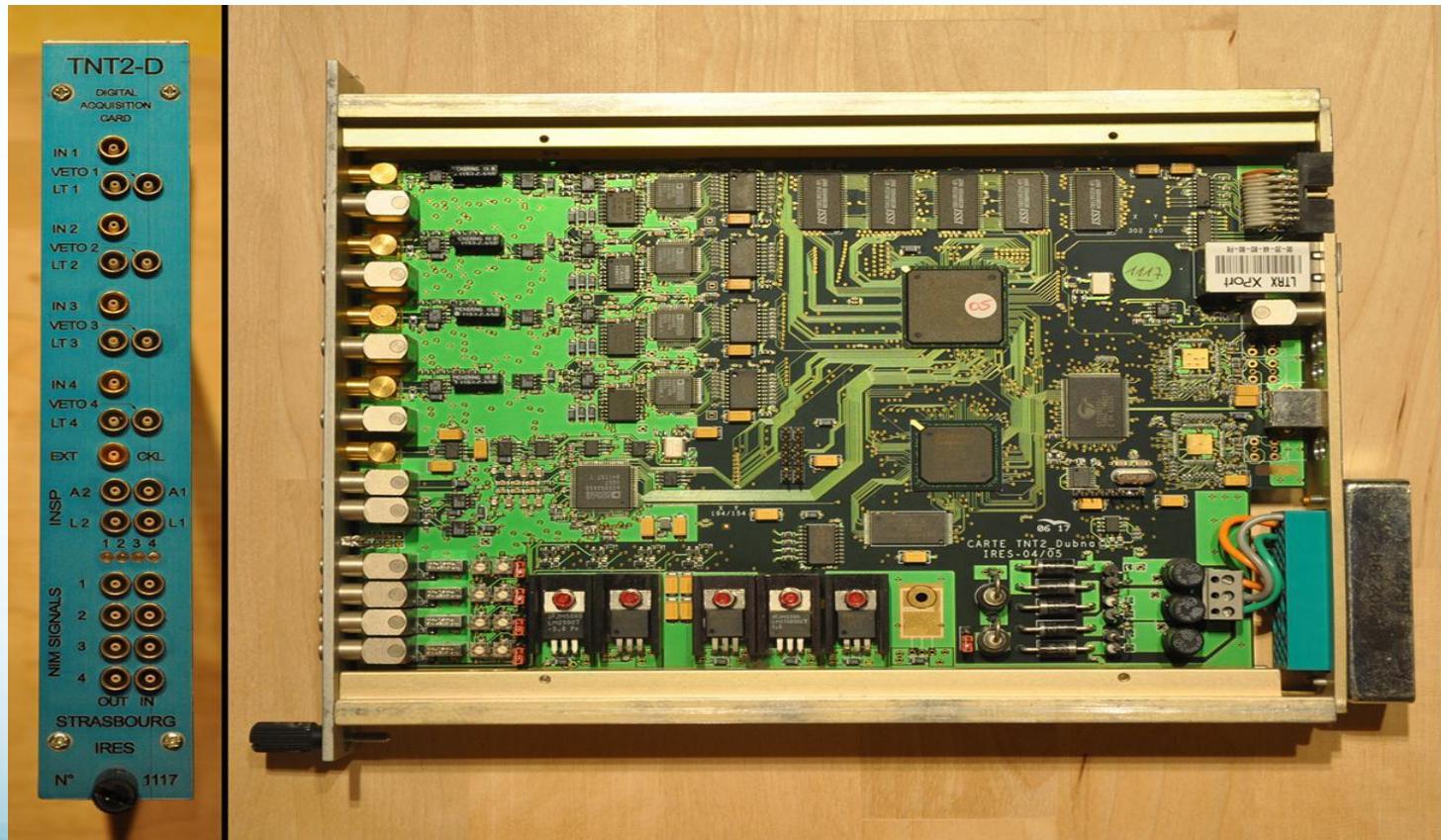
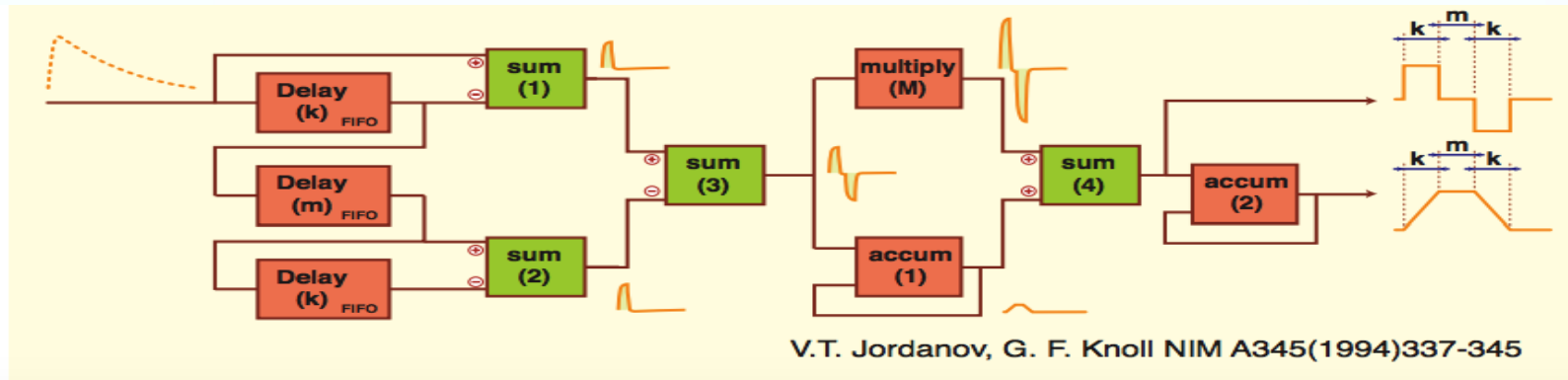


Figure 4. The TNT2 Card. /Courtesy of Benoît Gall

Introduction– The Jordanov Algorithm



$$d^{k,l}(n) = v(n) - v(n-k) - v(n-l) + v(n-k-l), \quad (1)$$

$$d^k(n) = v(n) - v(n-k), \quad (2)$$

$$d^{k,l}(n) = d^k(n) - d^k(n-l). \quad (3)$$

$$p(n) = p(n-1) + d^{k,l}(n), \quad n \geq 0, \quad (4)$$

$$r(n) = p(n) + Md^{k,l}(n), \quad (5)$$

$$s(n) = s(n-1) + r(n), \quad n \geq 0, \quad (6)$$

$$M = \frac{1}{\exp(T_{\text{clk}}/\tau) - 1}. \quad (7)$$

Results – Formation of the Jordanov Signals

- The principle behind the Jordanov pulse shaping is based on the following steps:
 1. First, we need to form the pre-amplification signal and make a fit with an exponential function in order to obtain a value for τ and a value for the amplitude of this pulse.

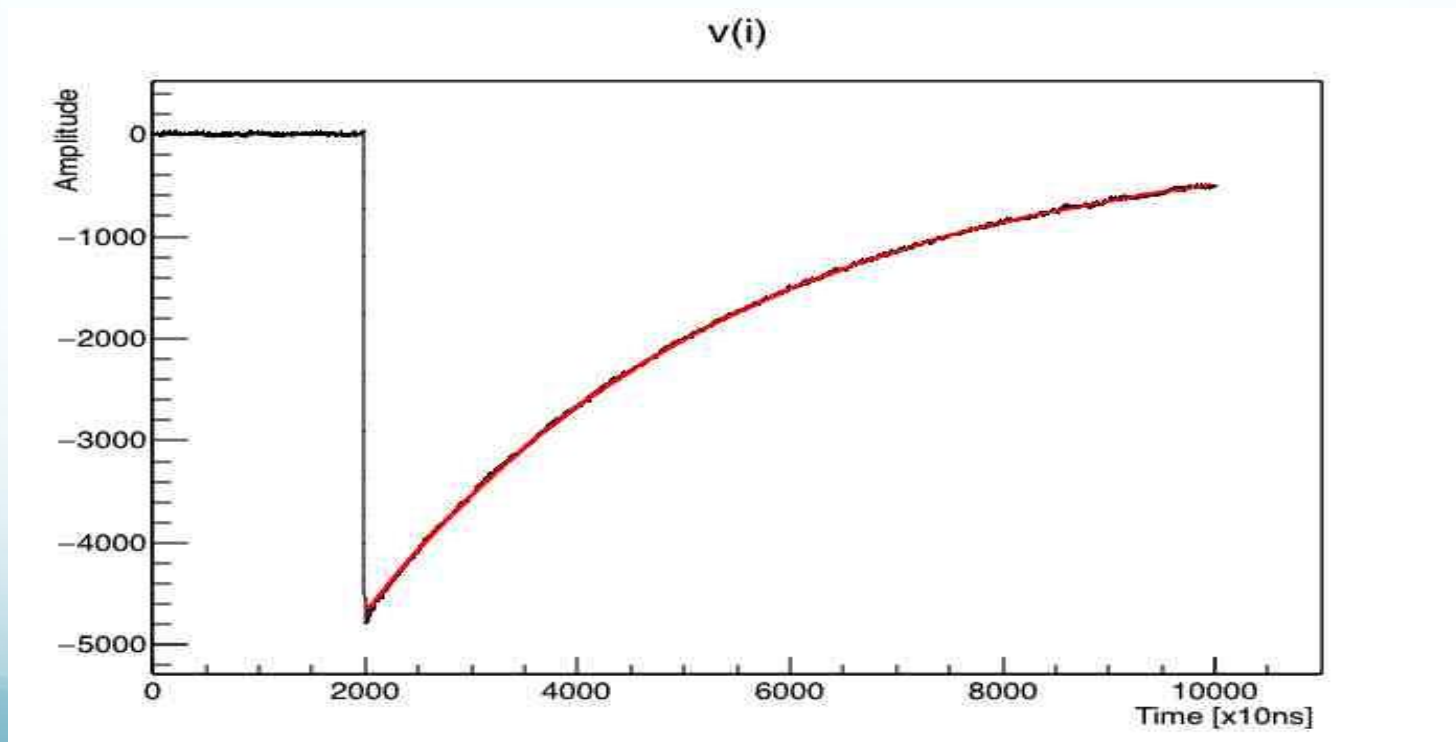
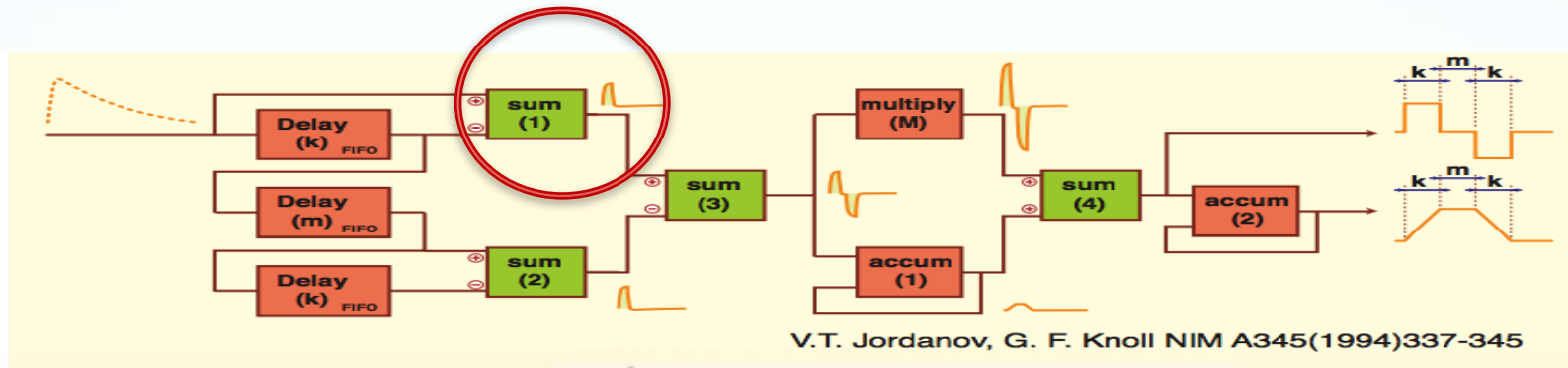


Figure 5. The digitized exponential pulse of the preamplifier. The red line stands for the fitting

Results– Formation of the Jordanov Signals



$$d^k(n) = v(n) - v(n - k),$$

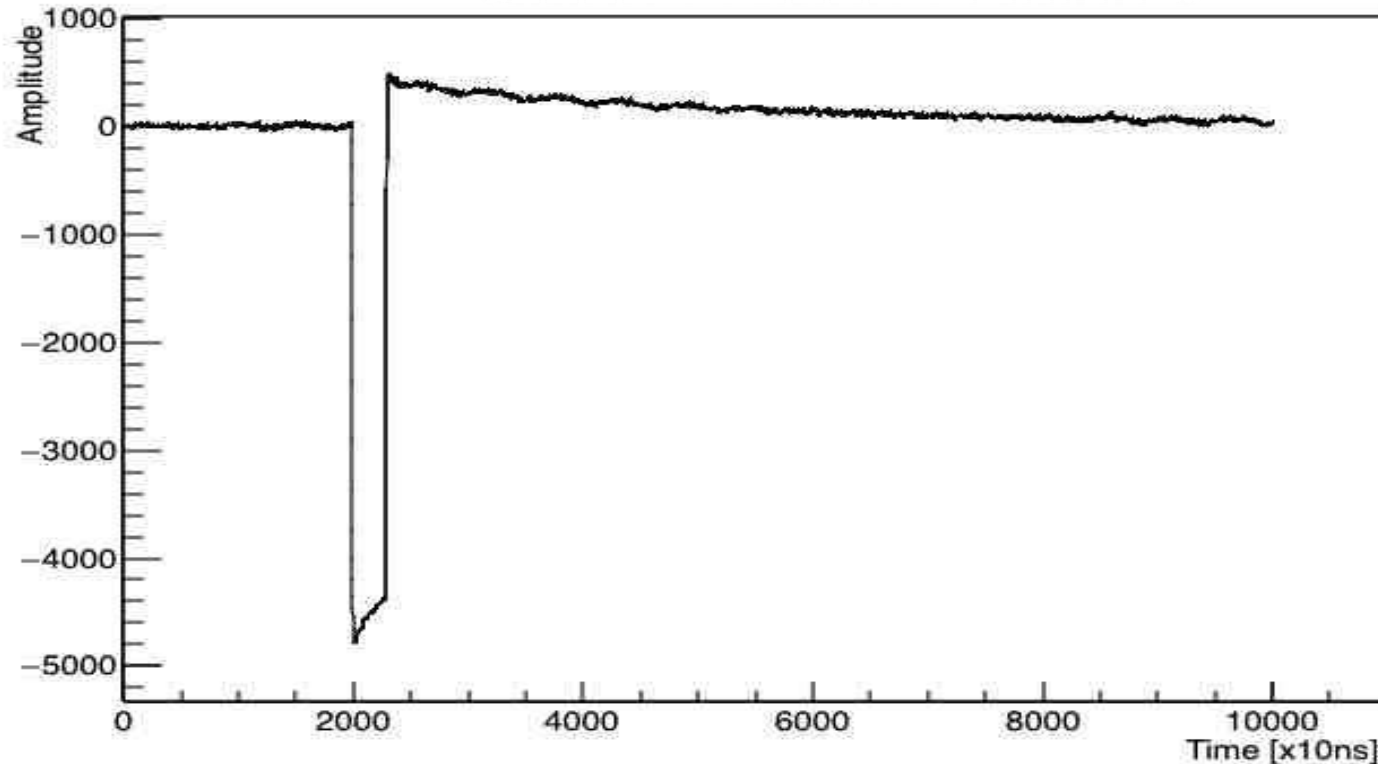
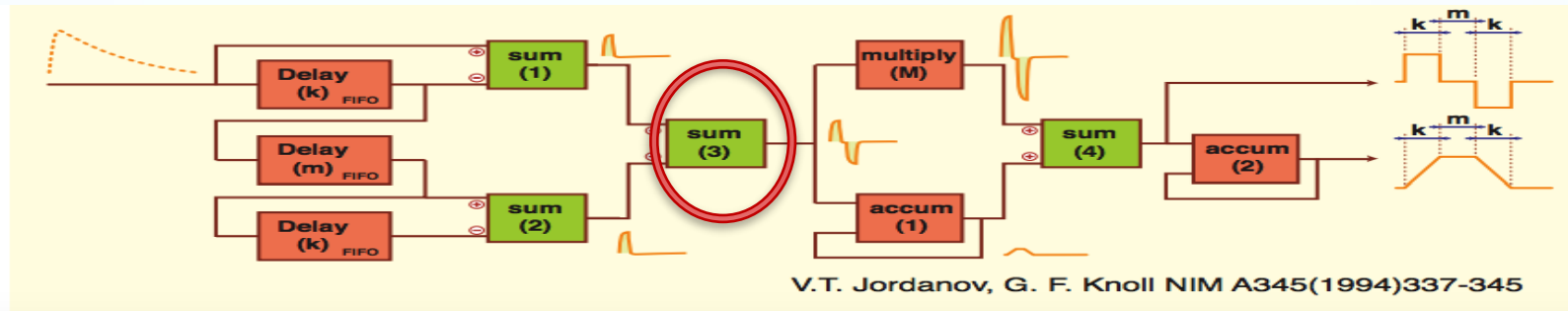


Figure 6. The signal after the implementation of the $d^k(n)$ algorithm.

Results– Formation of the Jordanov Signals



$$d^{k,l}(n) = v(n) - v(n-k) - v(n-l) + v(n-k-l),$$

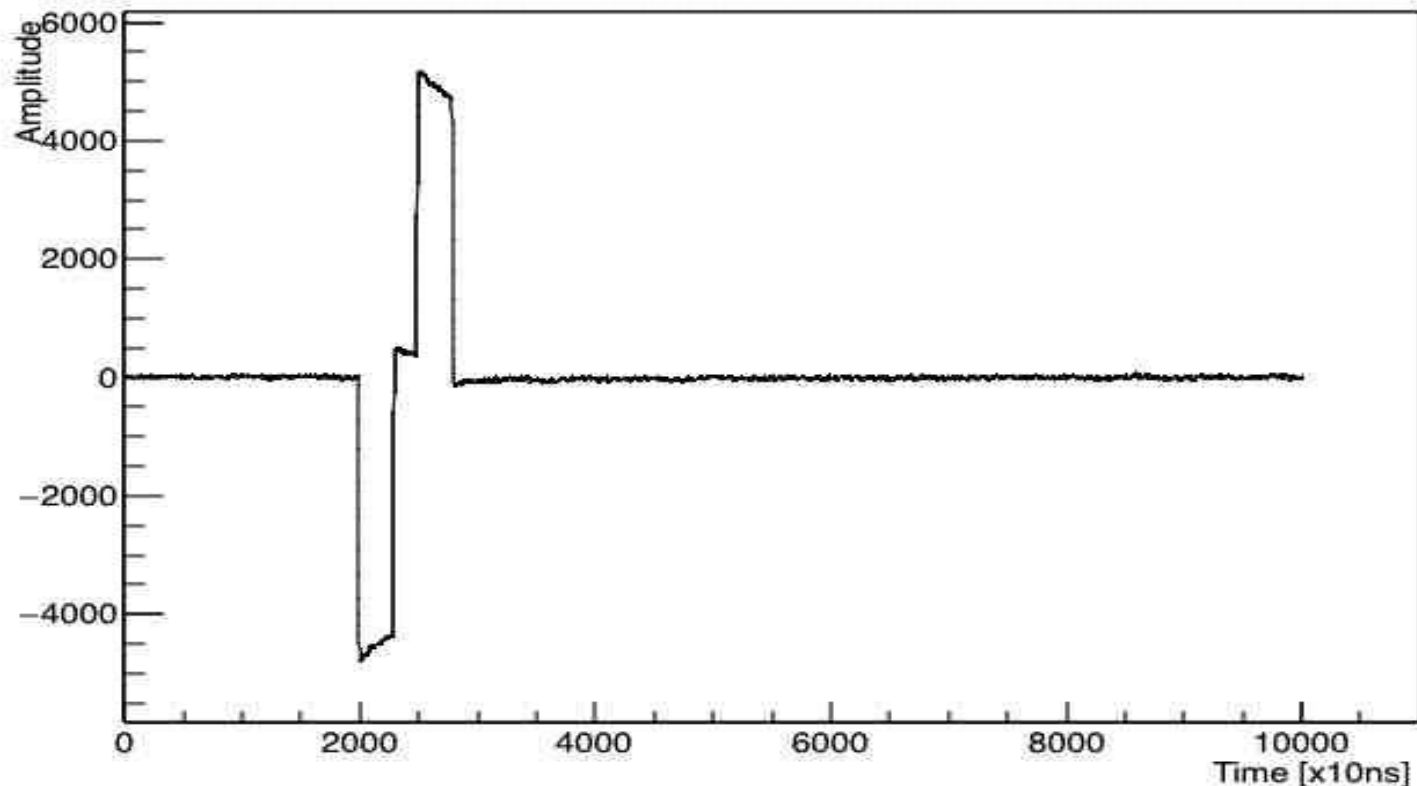
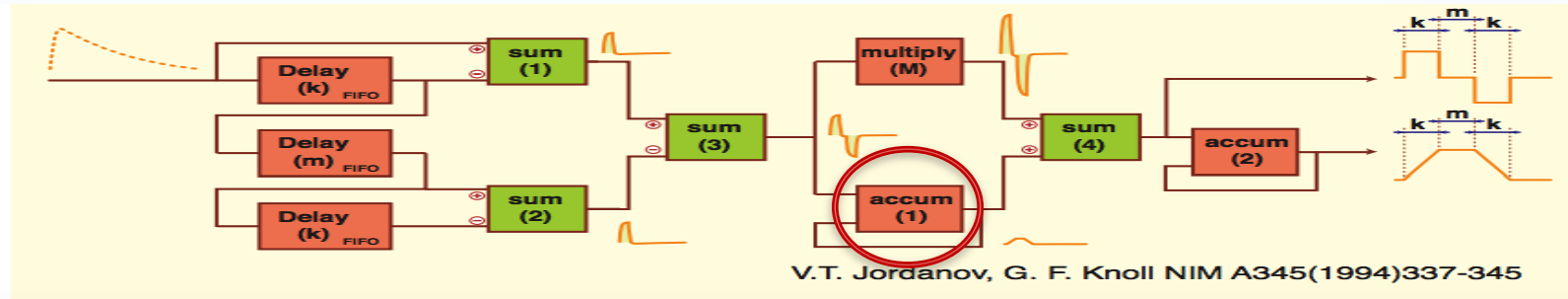


Figure 7. The signal after the implementation of the $d^{k,l}(n)$ algorithm.

Results– Formation of the Jordanov Signals



$$p(n) = p(n-1) + d^{k,l}(n), \quad n \geq 0,$$

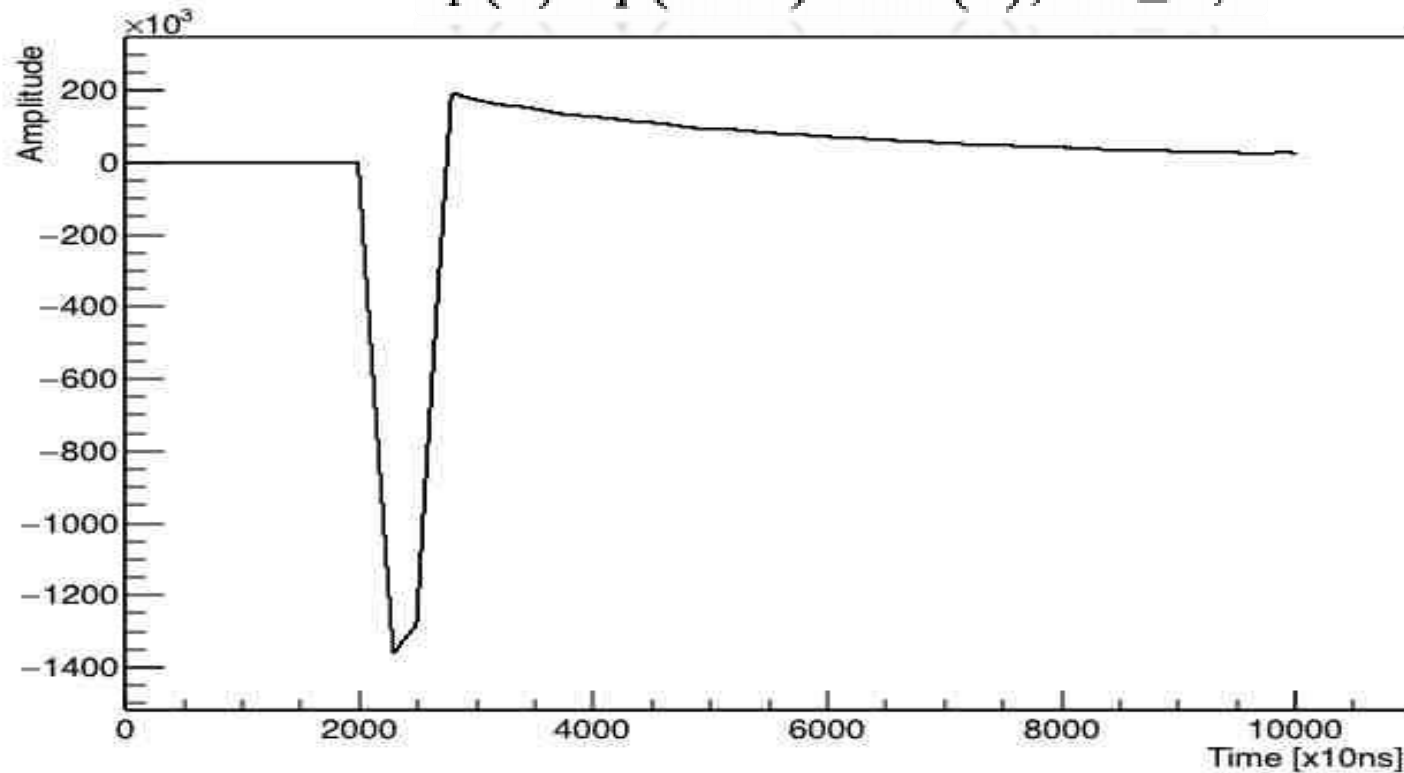
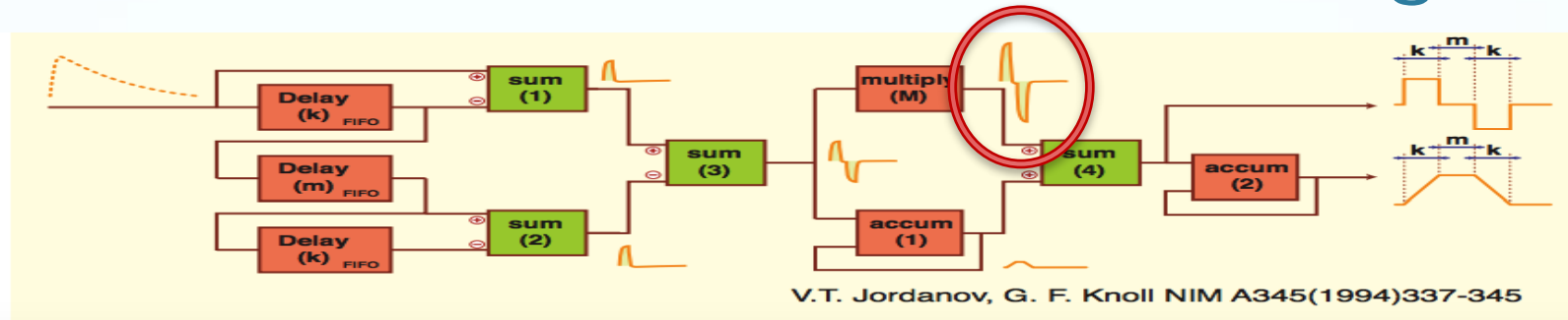


Figure 8. The signal after the implementation of the $p(n)$ algorithm.

Results– Formation of the Jordanov Signals



$$r(n) = p(n) + Md^{k,l}(n),$$

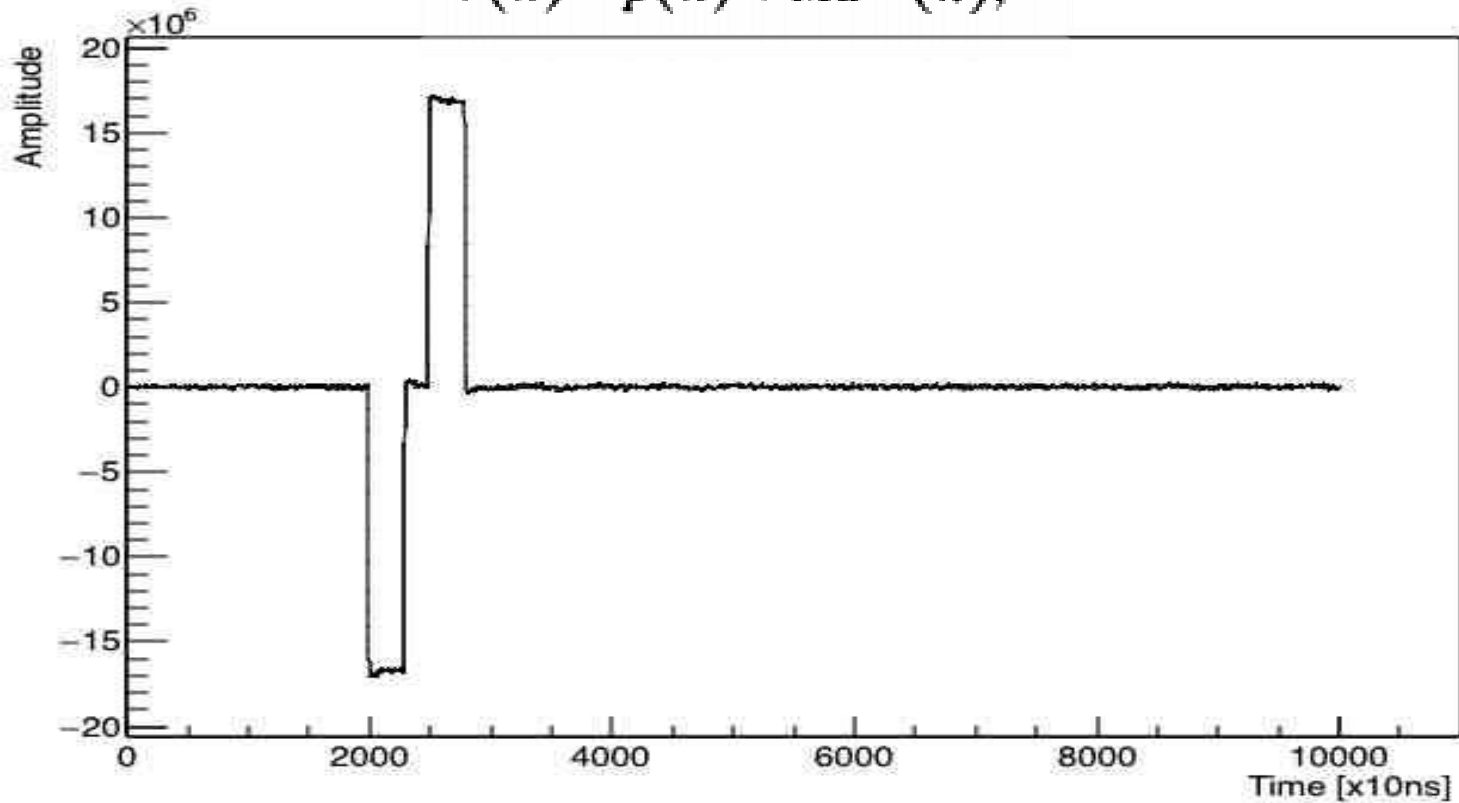
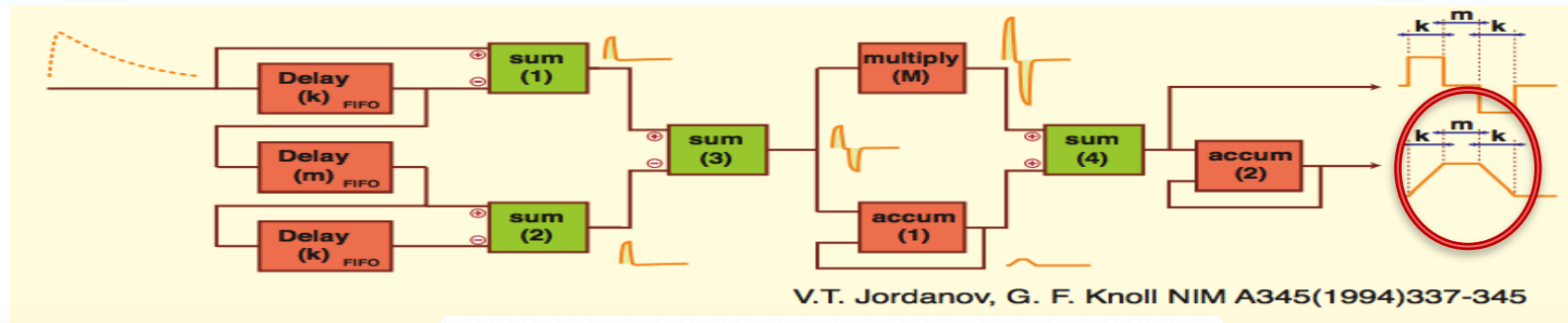


Figure 9. The signal after the implementation of the $r(n)$ algorithm.

Results– Formation of the Jordanov Signals



$$s(n) = s(n-1) + r(n), \quad n \geq 0,$$

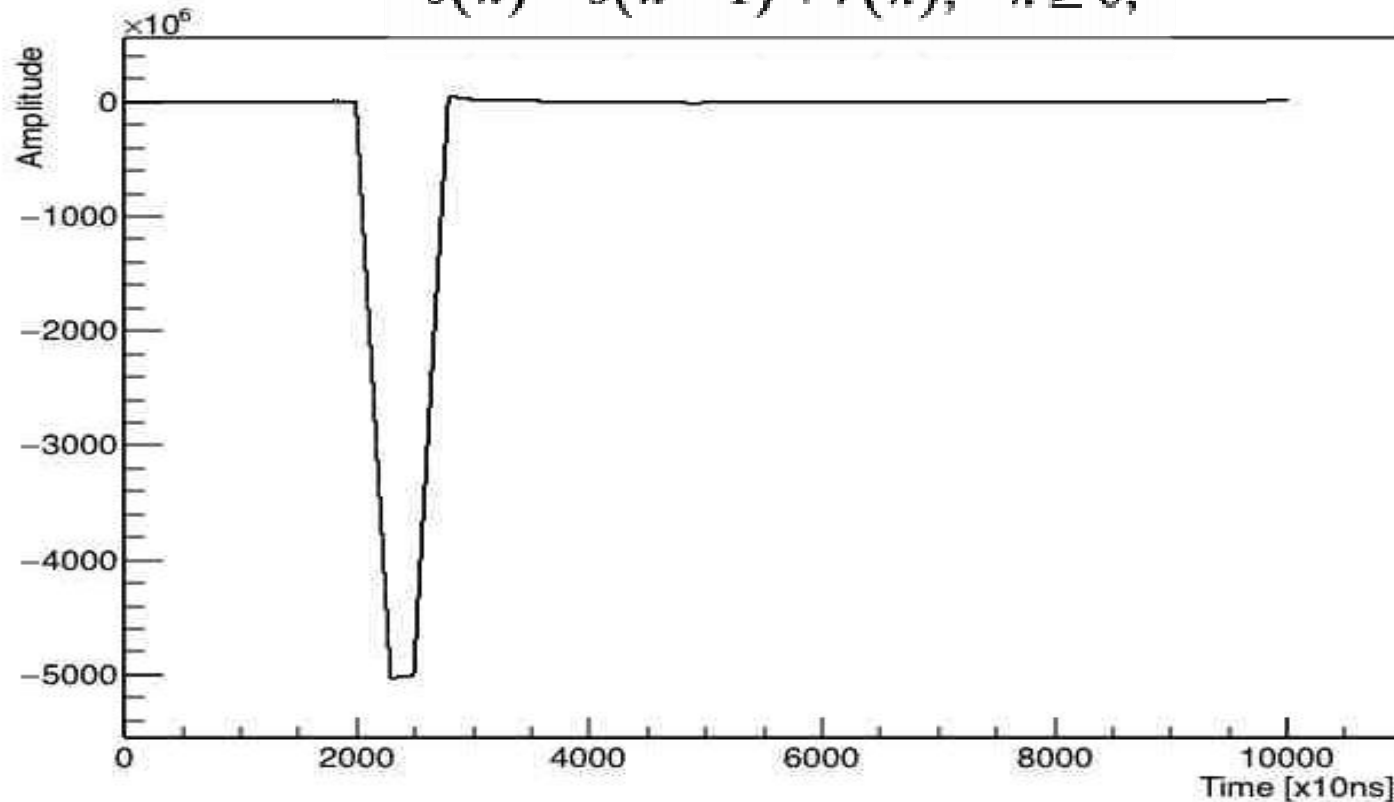


Figure 10. The signal after the implementation of the $s(n)$ algorithm.

Results– Role of M

- Parameter M depends only on the sampling period (T_{clk}) and on the decay time constant (τ). Since the sampling period remains the same, its value depends only on τ .
- M parameter plays an important role on the shaping of the trapezoidal pulse.

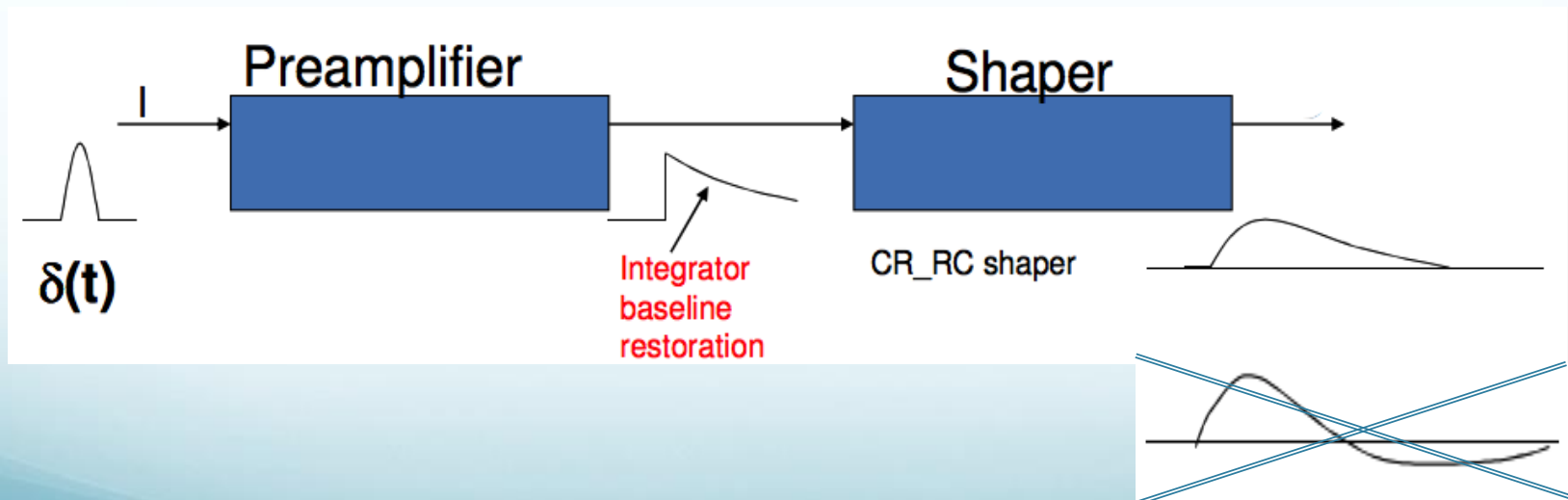


Figure 11. Readout Electronics: the role of M parameter/Silicon Strip Detectors and their electronics, Francis Anghinolfi, CERN

Results– Role of M

- The optimum value of M can restore the baseline of the pulse, fixes the undershoot and prevents a pile – up pulse.
- Eventually, we obtain a symmetrical trapeze from which we can measure the amplitude correctly.

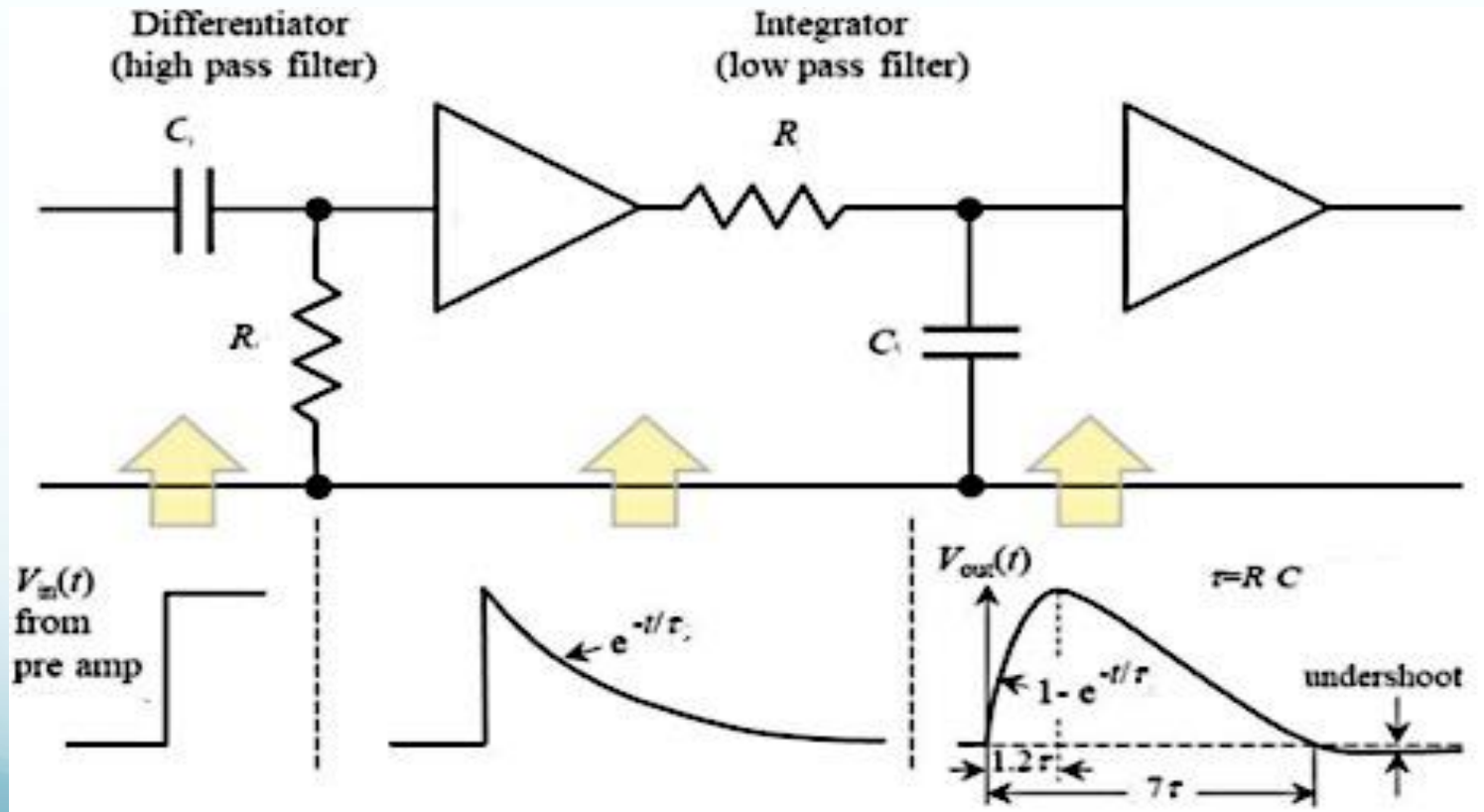


Figure 12. Basic shaping amplifier based on CR-RC filtering. The input pulse shape assumed to be a step function. / Semiconductor Radiation Detectors, Alan Owen

Results– Role of τ

- By changing the values of τ , the signals that are directly influenced are the $r(n)$ and $s(n)$, since they contain τ indirectly, through M parameter.
- By increasing the value of τ : the value of M decreases. The following graphs correspond to the values $\tau=17700$, 27700 ns and channel 3, accordingly.

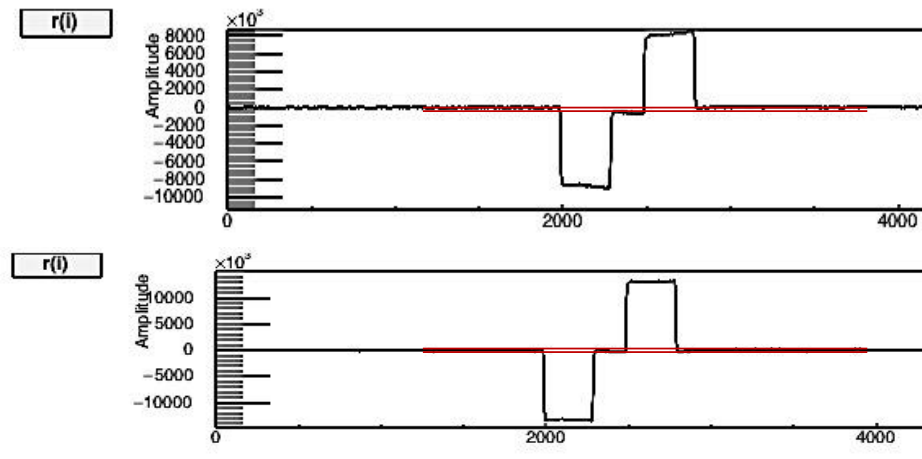


Figure 13. Different graphs of $r(n)$ signal after the implementation of different τ values.

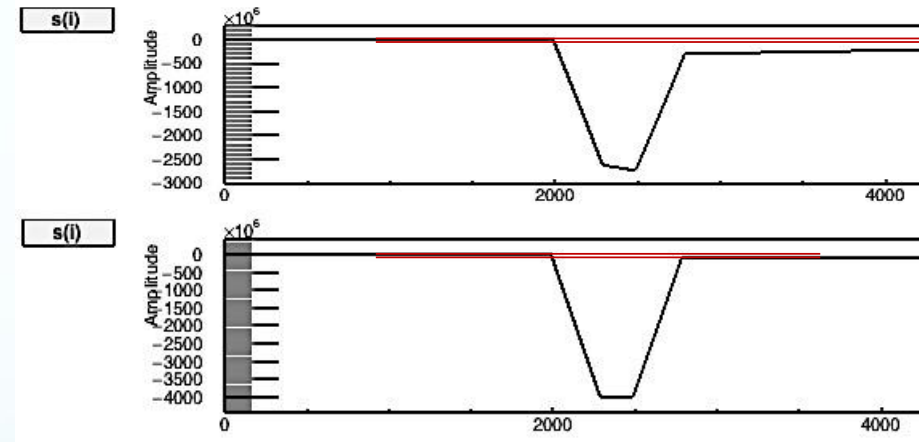


Figure 14. Different graphs of $s(n)$ signal after the implementation of different τ values.

Results– Tau Histograms

- They are filled with the τ values obtained automatically from the fitting of each exponential signal of every trace for every channel.
- With the implementation of the optimum tau value inside the code, we can obtain the optimum value of the M parameter and, therefore, a symmetrical trapezoidal shape and a correction of the undershoot.

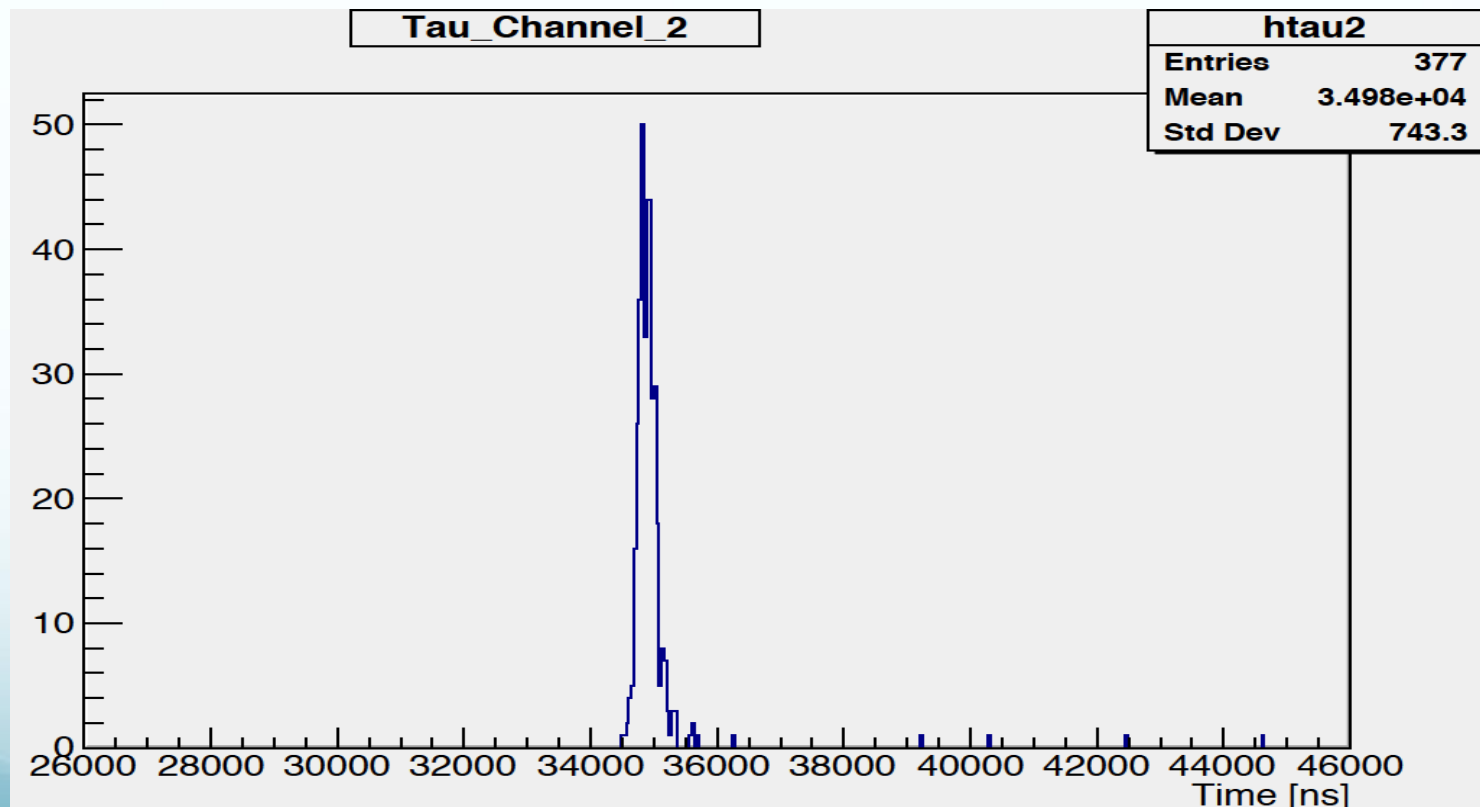


Figure 15. Histogram of tau values for channel 3.

Results – Amplitude Histograms

- They are filled with the values of amplitude that are calculated via the subtraction of the average Jordanov background and the average Jordanov plateau, inside the code.
- For every channel we obtain one histogram with three peaks which correspond to an energy value.

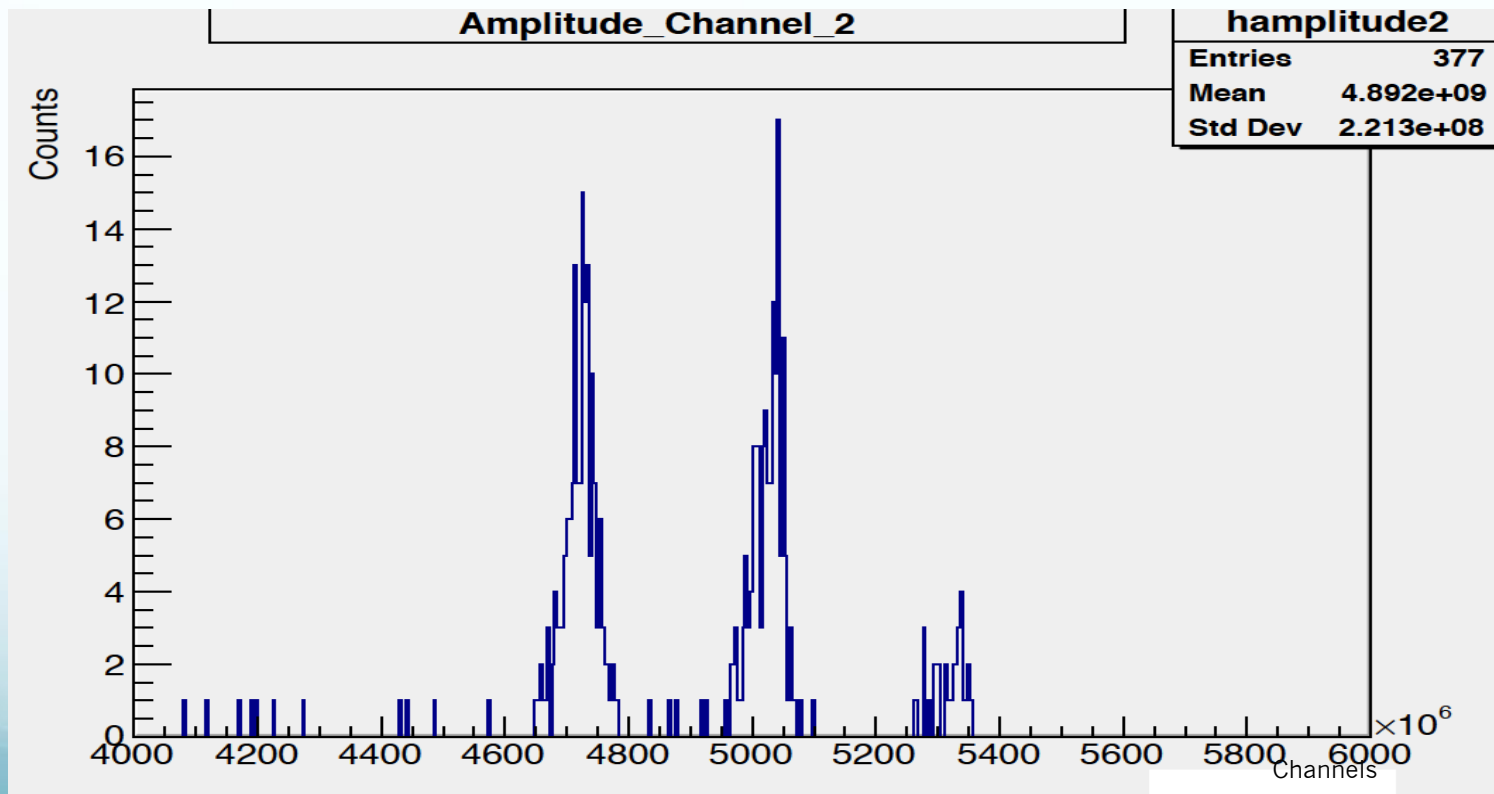


Figure 16. Histogram of amplitude values for channel 3.

Results – Energy Calibration

- Like the input signal, for which the amplitude is proportional to the deposited number of charges, the height of the trapezoid gives us the amplitude, in other words, the deposited energy after the calibration.
- The fitting aims to the extraction of the mean peak values and to their comparison with the tabulated ones.

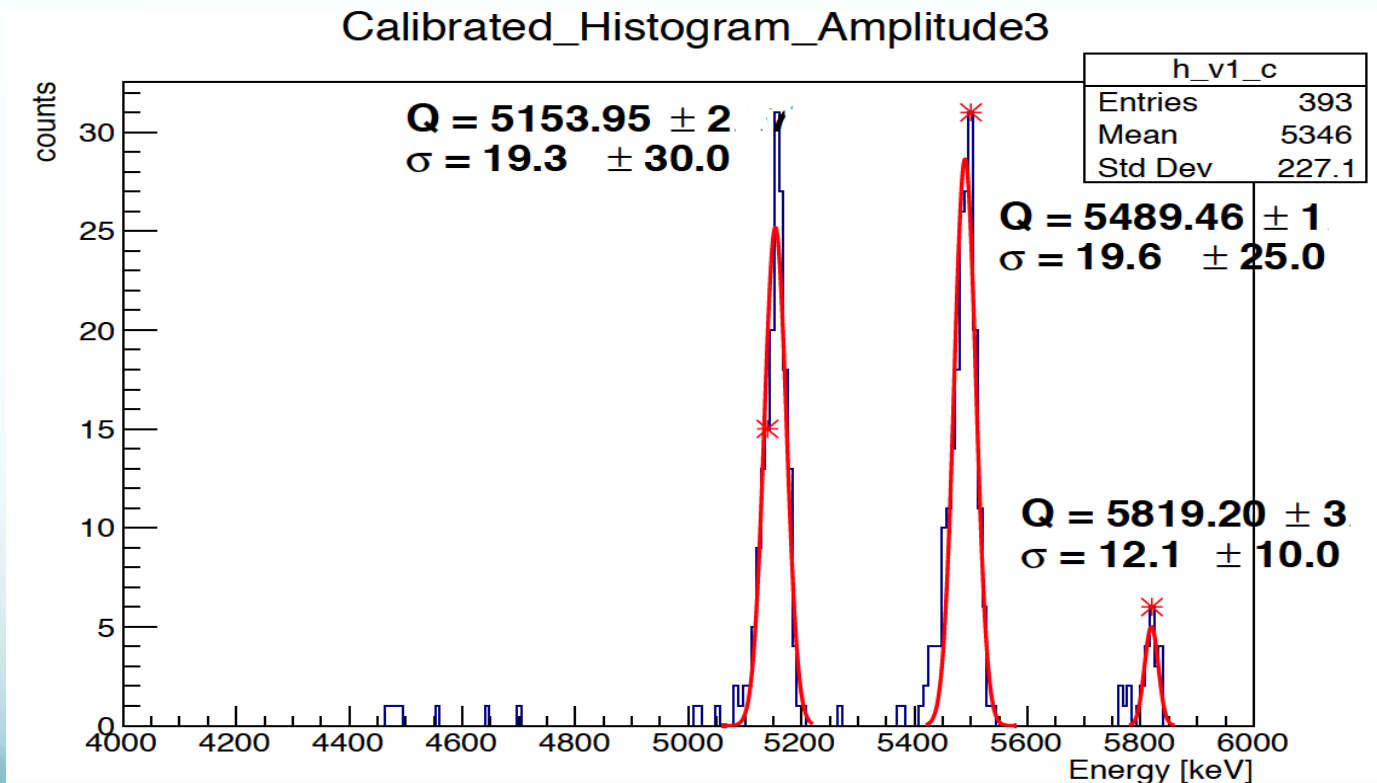


Figure 20. Histogram of amplitude values for channel 3.

Results – Energy Calibration

Calibrated_Histogram_Amplitude0

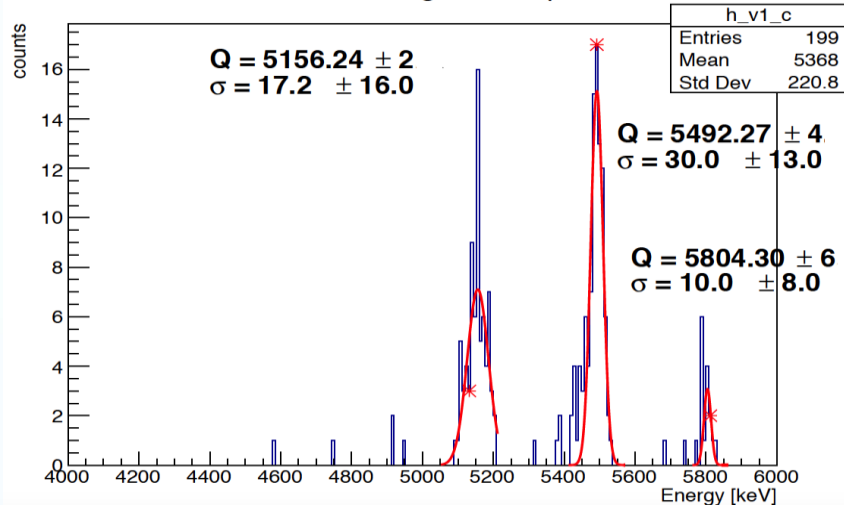


Figure 21. Histogram of amplitude values for channel 1.

Calibrated_Histogram_Amplitude1

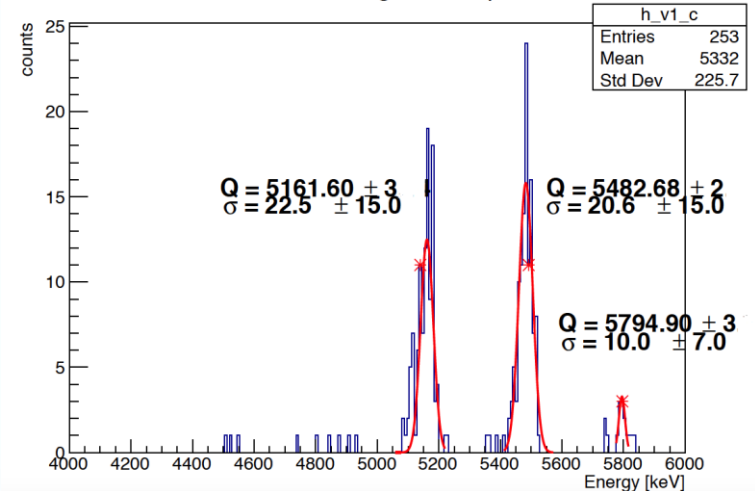


Figure 22. Histogram of amplitude values for channel 2.

Calibrated_Histogram_Amplitude3

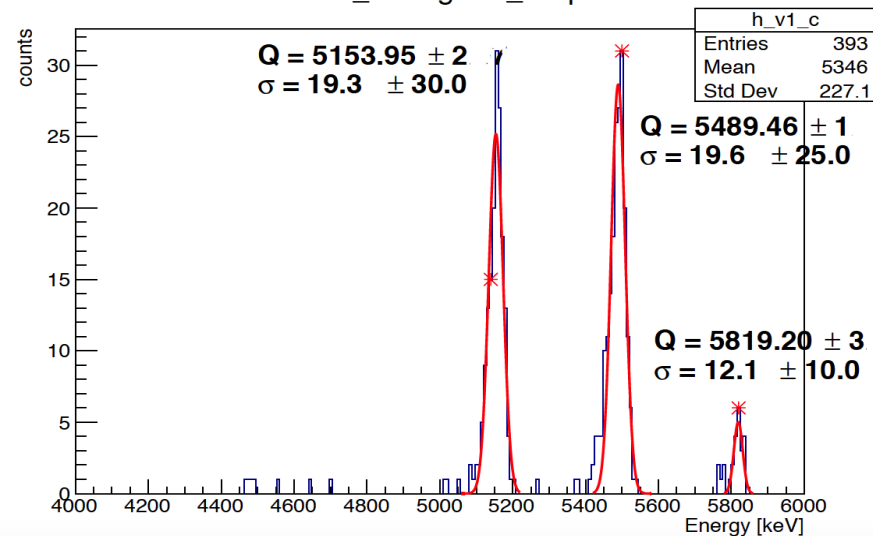


Figure 23. Histogram of amplitude values for channel 4.

Conclusion

- The implementation of the Jordanov algorithm provided us with knowledge around the pulse shaping and its importance on the reduction of noise on the signal.
- The understanding of the Jordanov shaping parameters and the way that they affect the signals, led us to the construction of the correct pulse waves.
- From the acquisition of the trapezoidal signal and the calculation of its background and plateau, we managed to obtain the histograms corresponding to the amplitude values from all the channels of the TNT2 card.
- The construction of the energy histogram and the following calibration, helped us relate the experimental energy values with the tabulated ones.

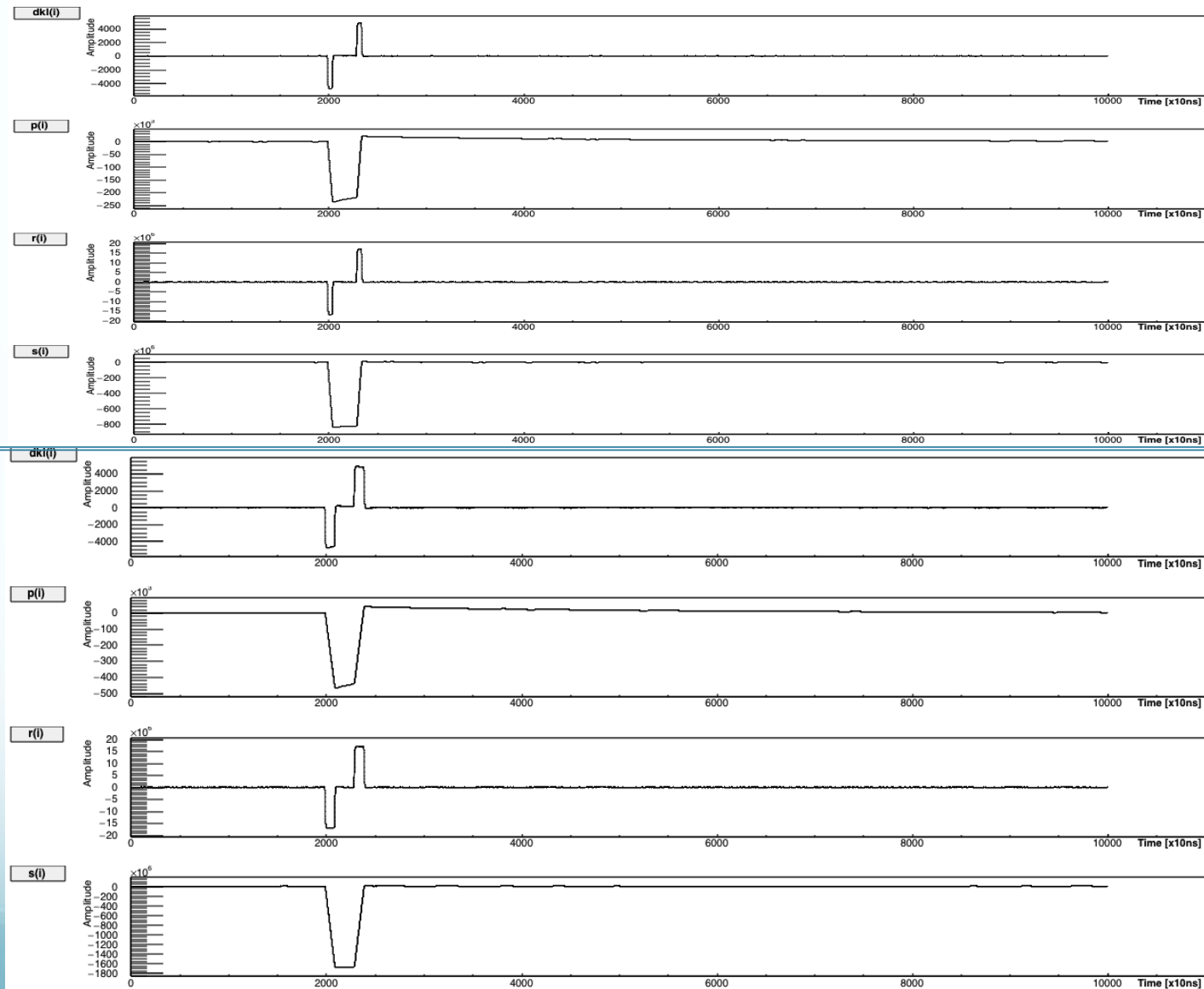
References

- [1] <http://www.iphc.cnrs.fr/-SPIRAL-2-.html>
- [2] <https://fr.wikipedia.org/wiki/SPIRAL2>
- [3] H. Faure. Développement et validation d'un nouveau détecteur silicium de grande taille pour S3-SIRIUS. Thèse présentée pour obtenir le grade de Docteur de l'Université de Strasbourg. September 2015.
- [4] P. Brionnet. Etude des états isomères des noyaux superlourds : ^{257}Db et ^{253}Lr . Thèse présentée pour obtenir le grade de Docteur de l'Université de Strasbourg.
- [5] V. Jordanov, G.F. Knoll, A.C. Huber, J.A. Pantazis. Digital Techniques for real – time pulse shaping in radiation measurements. Nuclear Instruments and Methods in Physics Research A 353 (1994) 261 – 264. Elsevier.
- [6] G. Knoll. Radiation Detection and Measurement .Third Edition. John Wiley & Sons, Inc. Editions.
- [7] EG&G ORTEC (1991/92). Semiconductor Radiation Detectors. CRC Press, Taylor&Francis Group.
- [8] A. Owens. Detectors and Instruments for Nuclear Spectroscopy, Preamplifier Introduction. Oak Ridge, USA.
- [9] F. Anghinolfi. Silicon Strip Detectors and their electronics, CERN
- [10] A. Owens. Semiconductor Radiation Detectors. CRC Press

Thank you for your attention!

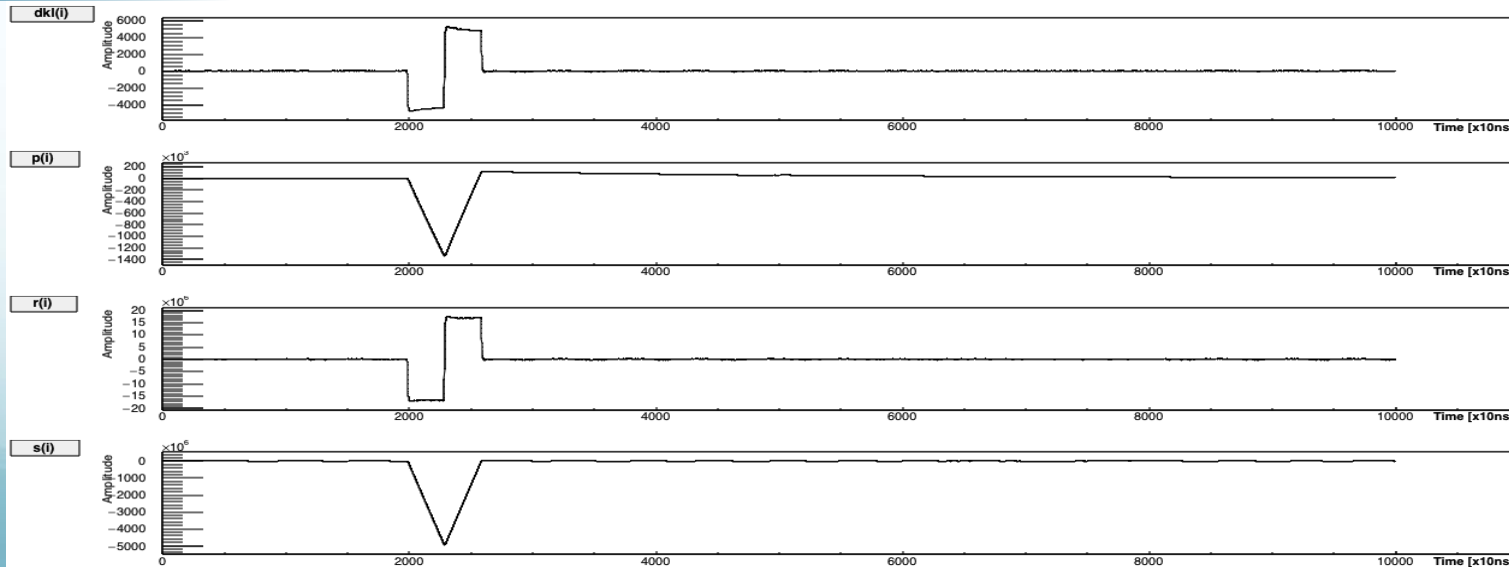
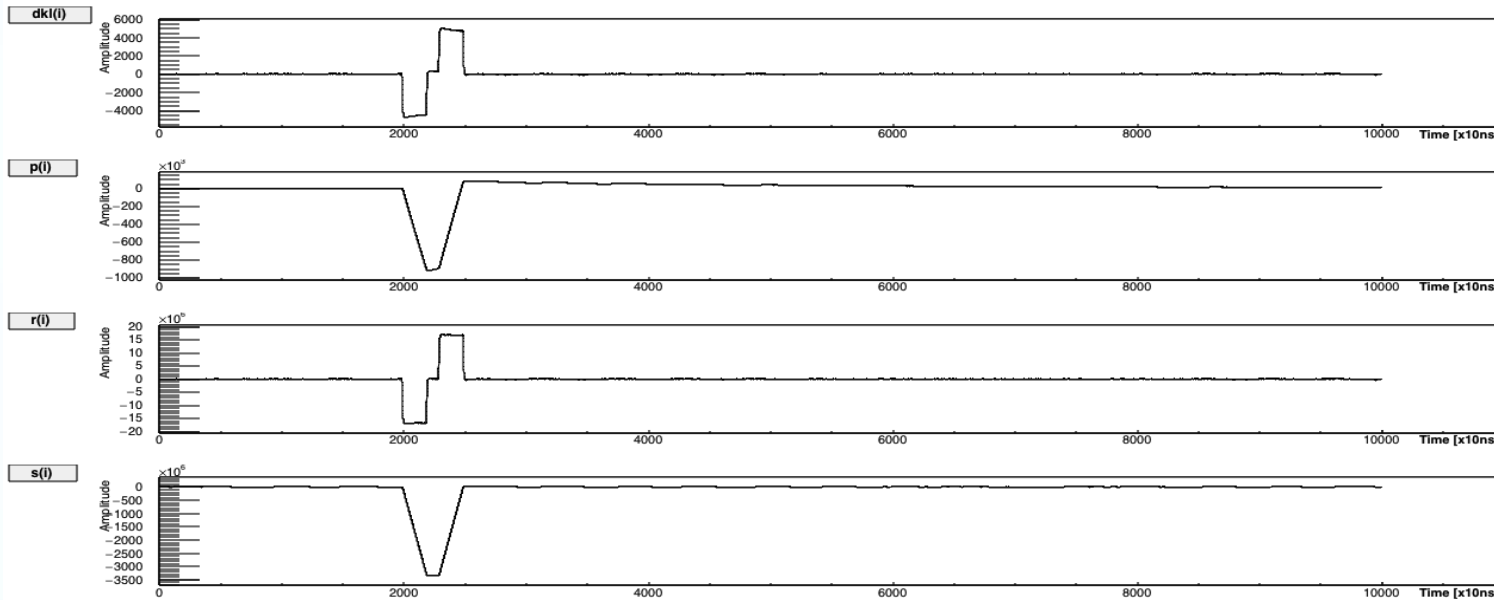
Backup Slides

- For $k=50,100$ and $l=300$ we obtain the following graphs.



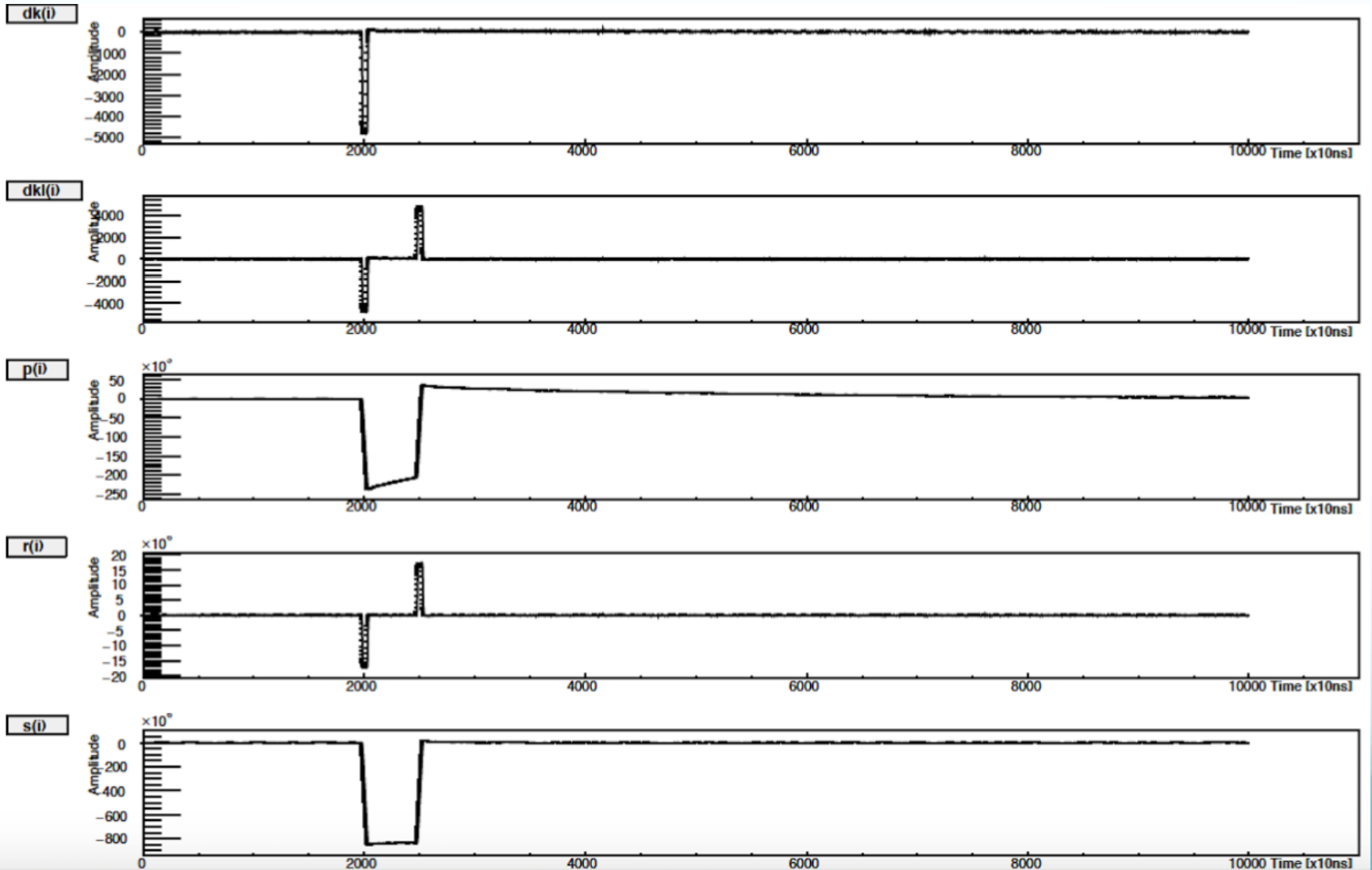
Backup Slides

- For $k=200,300$ and $l=300$ we obtain the following graphs.



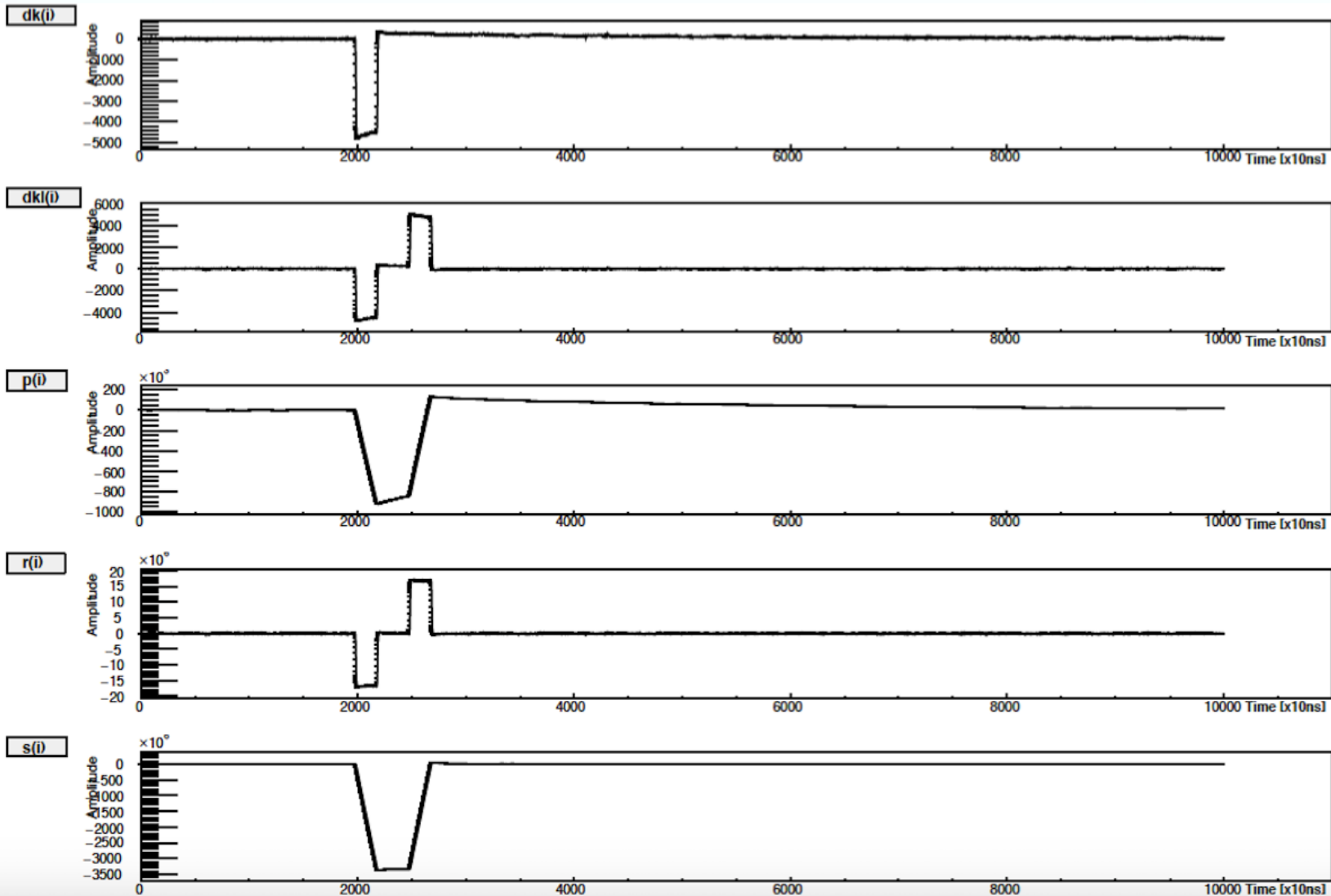
Backup Slides

- For $k=500$ and $l=50$ we obtain the following graphs.



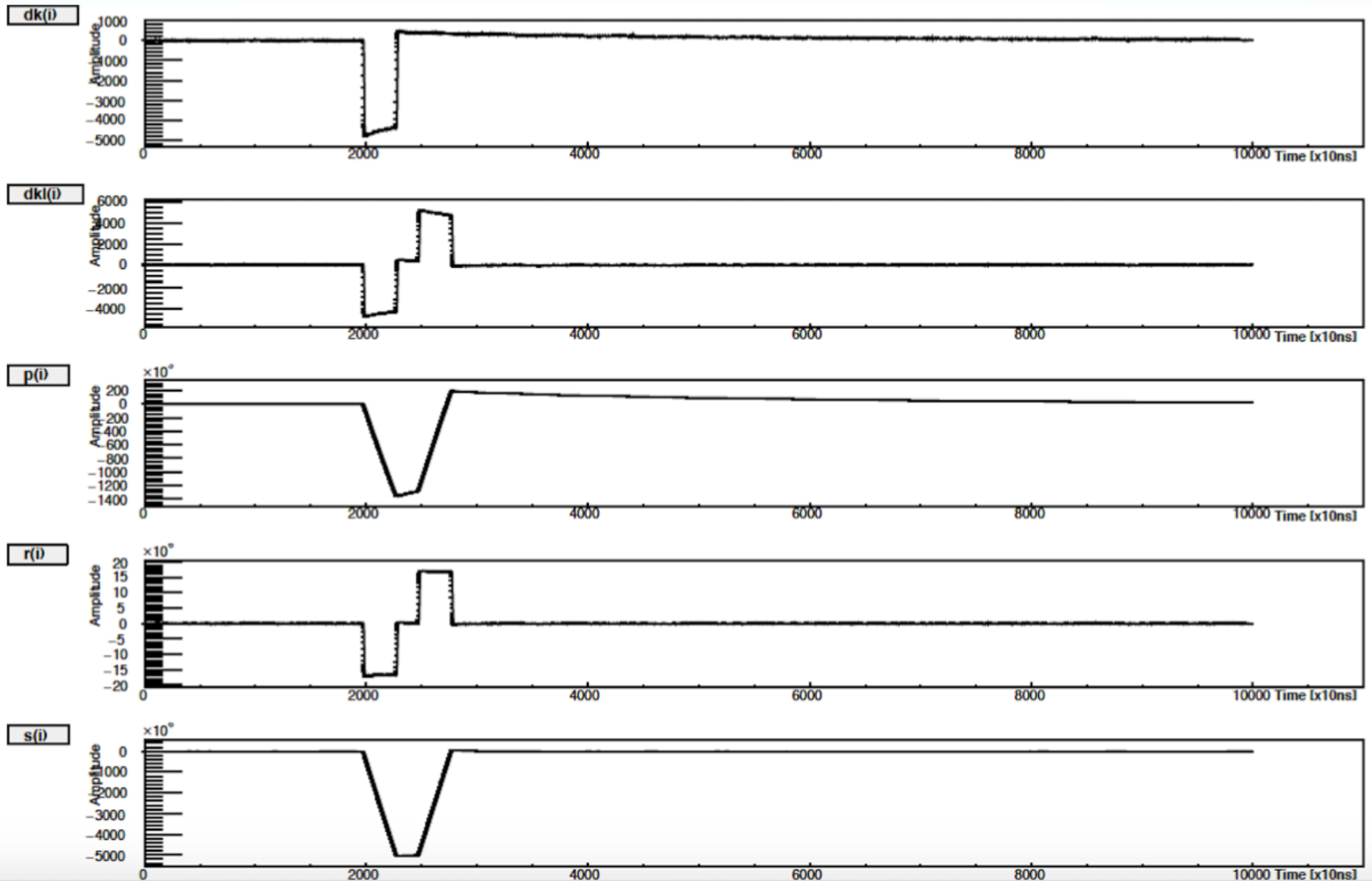
Backup Slides

- For $k=500$ and $l=200$ we obtain the following graphs.



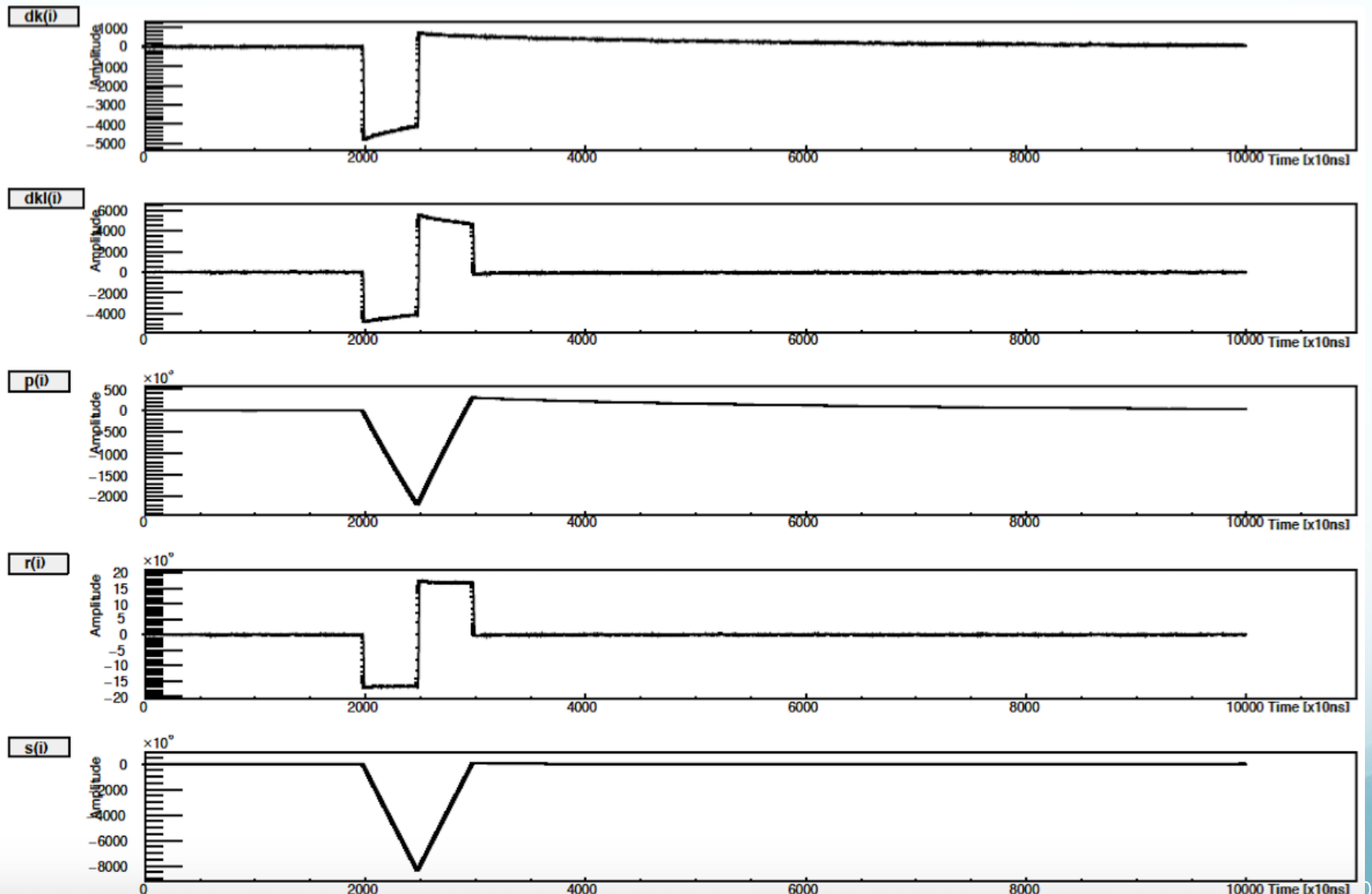
Backup Slides

- For $k=500$ and $l=300$ we obtain the following graphs.



Backup Slides

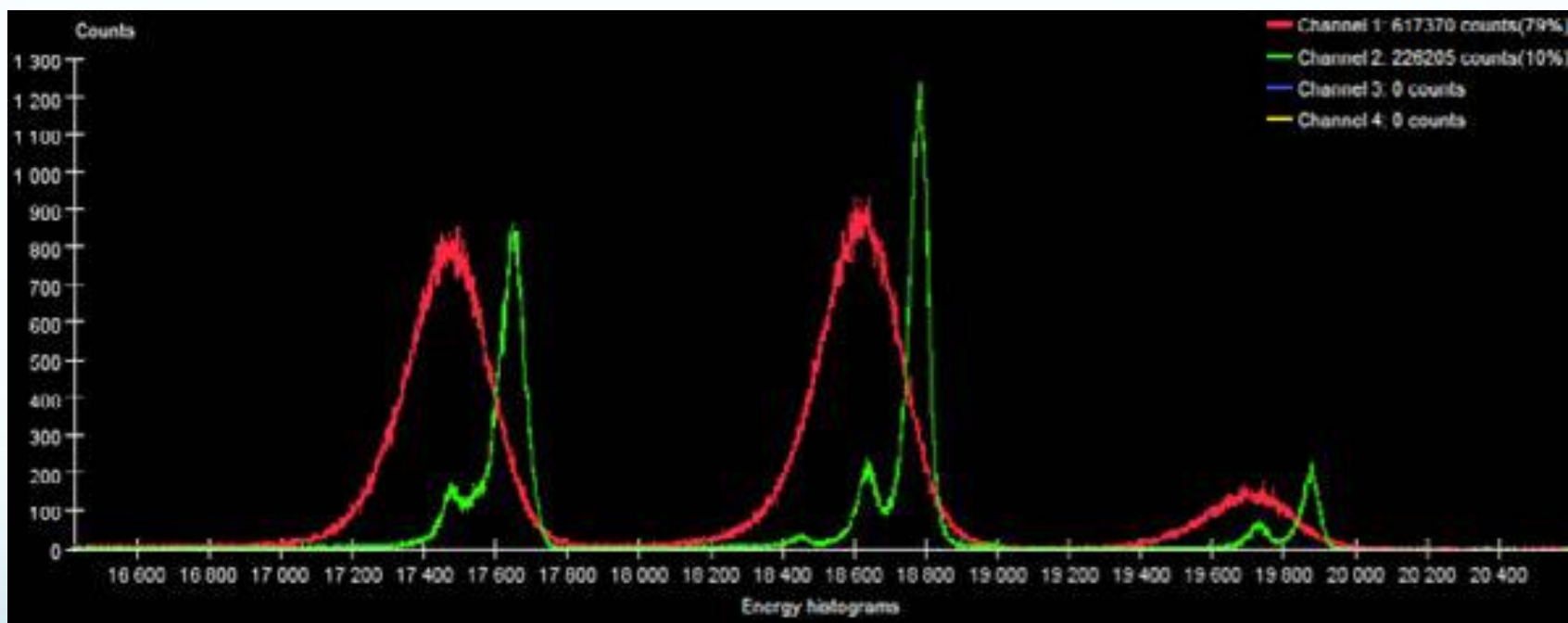
- For $k=500$ and $l=500$ we obtain the following graphs.



Backup Slides

- By changing the values of k and l parameter, the shapes of the Jordanov signals are influenced.
- When k is increasing, the amplitude of $p(n)$ and $s(n)$ is decreasing and the amplitude of $r(n)$ remains relatively stable but we observe a change in the x-axis since the value of $(l-k)$ is changing as well.
- When l is increasing, the amplitude of $p(n)$ and $s(n)$ is decreasing.

Backup Slides



Backup Slides

